Syntheses of Aluminosilicate Mesostructures with High Aluminum Content

Sophie Biz

School of Mechanical Engineering, Georgia Institute of Technology, Atlanta, Georgia 30332

Mark G. White*

School of Chemical Engineering, Georgia Institute of Technology, Atlanta, Georgia 30332-0100

Received: December 14, 1998; In Final Form: February 24, 1999

Ordered aluminosilicate mesostructures having a SiO_2/Al_2O_3 ratio near 5 were prepared using a surfactant-templated synthesis. The solid structures were analyzed by scanning electron microscopy (SEM), nitrogen sorption to determine pore volume and pore sizes, powder X-ray diffraction (PXRD), thermal desorption of a chemisorbed base to determine strong acid site density, and magic-angle-spinning (MAS) NMR spectroscopy for the ^{27}Al and ^{29}Si nuclei. We were successful in synthesizing a mesoporous aluminosilicate having a SiO_2/Al_2O_3 ratio near 5 when the source of the aluminum ion was Al hydroxide and the surfactant was cetyltrimethylammonium cation ($C_{16}TMA^+$). The uncalcined samples showed only tetrahedral aluminum as confirmed by ^{27}Al MAS NMR. When the pH of the synthesis gel was 10.5, the mesostructure developed a pore volume of 0.59 cm^3/g with an average pore diameter of 2.2 nm. The pore volume was less at pH values other then 10.5 (e.g., for pH 12.6 and 8.1, the pore volumes were 0.50 and 0.43 cm^3/g, respectively). The aluminosilicate mesostructure showed Brønsted and Lewis sites as confirmed by the IR vibrational spectroscopy of chemisorbed pyridine. The mesostructure Brønsted acid site density was 0.36 μmol H^+/m^2-solid, based on Brønsted acid site titration by isopropylamine temperature-programmed desorption. It was similar to that observed for an amorphous alumina−silica having a SiO_2/Al_2O_3 ratio near 6. However, the mesostructure Brønsted site density per unit mass was much lower than that measured for an acidic Y-faujasite with a SiO_2/Al_2O_3 ratio of 2.75.

Introduction

In recent years, the necessity to treat heavier feeds and process large molecules has created a demand for molecular sieves with pores larger than those zeolites have. The disclosure of MCM-41 surfactant-templated mesostructures[1,2] by Mobil researchers in 1992 offered the prospect to extend existing catalytic and sorption processes to molecules having dimensions in the mesoporous range (between 2 and 50 nm). In particular, it would be of interest for the petrochemical industry to synthesize a catalyst that combines the acid site strength and the hydrothermal stability of zeolite cracking catalysts with the narrow pore size distribution of MCM-41 mesostructures.[1,2] It is possible to incorporate small quantities of aluminum in the framework of MCM-41 by direct synthesis in order to create acidic sites.[3−9] However, attempts were unsuccessful to synthesize MCM-41 from gels having a SiO_2/Al_2O_3 ratio below 10, as the final products generally possess a wide distribution of pore sizes and the structure shows an amorphous powder X-ray diffraction pattern.[3,9]

It is the purpose of this article to report the synthesis of ordered aluminosilicate mesostructures with a SiO_2/Al_2O_3 near 5, using a surfactant-templated synthesis mechanism. The effects of Al source and synthesis pH on the solid structure and surface acidity are discussed. The structural and acidic properties of the aluminosilicate mesostructures are compared with the properties of two aluminosilicate catalysts with a high Al content: AAA Alumina (an amorphous alumina−silica mixture with $SiO_2/Al_2O_3 \sim 6.2$, obtained from the American Cyanamid Co.) and acidic faujasite (zeolite HY with $SiO_2/Al_2O_3 = 2.75$, CBV 712, obtained from PQ Corp.) that are used as components of fluid cracking catalysts in industry.

Synthesis

Starting Materials. We selected two different silicon precursors to make the hydrogels: (1) tetraethyl orthosilicate, $(C_2H_5O)_4Si$, from Fisher Scientific (Norcross, GA) and (2) colloidal silica, Ludox AS-40, from E. I. DuPont. Three different aluminum precursors were used: (1) Al isopropoxide, $Al(OC_3H_7)_3$ (98%+ purity from Aldrich, Inc); (2) Na aluminate ($NaAlO_2$ (8 wt % H_2O) from Strem Chemicals (Newburyport, MA); and (3) Al hydroxide, $Al(OH)_3$, from Pflatz and Bauer, Inc. The organic base, tetraethylammonium (TEA^+) hydroxide (20 wt % in water), was secured from Sachem, Inc., and the surfactant, cetyltrimethylammonium chloride ($C_{16}H_{33}(CH_3)_3N^+Cl^-$, 25 wt % in water), was obtained from Aldrich Chemical Co. Deionized water was used in all of the preparations.

Procedure. *(a) Aluminosilicate MCM-41.* We attempted to prepare high Al content MCM-41 mesostructures using three different Al sources: Al hydroxide, Al isopropoxide, and Na aluminate.

Hydrogels of molar composition Al_2O_3:5.2SiO_2:3.3$[TEA]_2O$:4.7$[C_{16}TMA]_2O$:1000 H_2O were prepared as follows. The Al source was dissolved in tetraethylammonium hydroxide solution. The resulting solution was slowly added to tetraethyl orthosilicate together with the cetyltrimethylammonium chloride and excess deionized water. The resulting mixture was a yellow

10.1021/jp984790z CCC: $18.00
Published on Web 09/16/1999

transparent solution that turned to a white milky gel within 3−4 min. The final pH of this hydrogel was 12.8. After 1 h stirring at room temperature, the pH was lowered using 10% hydrochloric acid. The gel was heated to ~40 °C in order to vaporize the alcohol produced by alkoxide hydrolysis. It was then loaded into Teflon-lined autoclaves and heated at 110 °C for a week. The resulting solid products were recovered by filtration, washed several times with ~80 °C deionized water, and dried at 110 °C in air for 12 h. In order to remove the organic species that were residing in the pores, the solids were heated to 600 °C under a flow of nitrogen with a heating ramp of 2 °C/min. They were kept at 600 °C for 1 h under a flow of nitrogen and 6 h in air.

(b) Pure Silica MCM-41. An hydrogel of molar composition $33SiO_2$:$3.3(TEA)_2O$:$4.7(C_{16}TMA)_2O$:$1000\ H_2O$ was prepared by adding cetyltrimethylammonium chloride, tetraethylammonium hydroxide, and water to colloidal silica. The pH of the gel was 12.7. The resulting mixture was allowed to age at room temperature for 2 h with stirring. The gel was loaded in a Teflon-lined autoclave and heated to 110 °C for 3 days without stirring. The subsequent steps were the same as in procedure (a).

Ion Exchange. The calcined aluminosilicate mesostructures prepared from Na aluminate were ammonium-exchanged and calcined in air in order to remove the Na^+ species in ion-exchange positions and replace them with protons. Following a procedure typically used for zeolites, the crystal powder was dispersed in a 1 M NH_4NO_3 solution and stirred for 5 h at room temperature. The liquid volume to solid mass ratio was 100 mL/g. The ammonium-exchanged mesostructure, NH_4^+-MCM-41, was isolated by filtration. The protonic form, H^+-MCM-41, was obtained by heating the sample at 500 °C for 1 h in air with a heating ramp of 1 °C/min.

Structure Characterization

Chemical Analyses. Galbraith Laboratories Inc., Knoxville, TN, performed the chemical analyses for Si and Al.

Powder X-ray Diffraction. Powder X-ray diffractograms were collected on a Scintag diffractometer using Cu Kα radiation and a Scintag, Peltier-cooled, solid-state detector. Scans were run in continuous mode from $2\Theta = 1°$ to 10° at a speed of 1.0°/min.

N_2 Sorption. Pore volume, surface area, and pore size distribution was measured by nitrogen sorption at 77 K with an ASAP-2010 porosimeter from Micromeritics Corp. (Norcross, GA). Prior to analysis, the samples were degassed in a vacuum at 350 °C for at least 12 h. The mesopore volume was estimated from the amount of nitrogen adsorbed at a relative pressure of 0.5 by assuming that all the mesopores were filled with condensed nitrogen in the normal liquid state. This is a good approximation as long as (i) there are no micropores in the solid and (ii) the amount of nitrogen adsorbed on the external surface of the crystals is much lower than the amount of nitrogen condensed in the mesopores. Pore size distributions were estimated using the density functional theory (DFT Plus software, from Micromeritics) and the Barrett, Joyner, Halenda (BJH[10]) algorithm (ASAP 2010 built-in software, from Micromeritics). In the latter method, Harkins and Jura's thickness equation was used to estimate the thickness of nitrogen molecules adsorbed on the pore walls.

^{27}Al MAS NMR. Solid state ^{27}Al NMR measurements were performed on a Bruker DSX 300 spectrometer equipped with a magic-angle-spinning (MAS) unit. The ^{27}Al MAS NMR spectra were recorded at a frequency of 72.22 MHz and a spinning rate of 6 kHz, with a pulse length of 1.0 μs, a delay time of 0.2 s, a spectral width of 330 ppm, and 1024 scans. The line broadening was 50 Hz. The ^{27}Al chemical shifts were reported relative to a liquid solution of $Al(NO_3)_3$.

^{29}Si MAS NMR. ^{29}Si MAS NMR spectra were acquired on a Bruker DSX 300 spectrometer at a frequency of 59.64 MHz, using a spinning speed of 6 kHz, a pulse width of 2.50 μs (45° pulse), a delay time of 10 s, and a spectral width of 335 ppm. Two thousand (2000) scans were acquired, and processed with a line broadening of 50 Hz. The chemical shifts are reported with reference to trimethylsilylpropanesulfonic acid (TSP).

Acidity Characterization

Infrared Spectroscopy. The nature of the acid sites was probed by infrared spectroscopy (IR) with pyridine as the probe molecule. When pyridine is protonated on a Brønsted acid site, the pyridine aromatic ring shows a characteristic vibration near 1540 cm^{-1}. When pyridine is coordinatively bound to a Lewis acid site, it gives an infrared band between 1447 and 1460 cm^{-1}.[11,12] Prior to the experiment, pyridine was purified by the "freeze−pump−thaw" method, repeated two times. Then, the catalyst wafers were activated at 500 °C for 1 h in a vacuum (~5 μmHg). The cell was cooled to 150 °C and a reference spectrum was collected at this temperature. Pyridine was then admitted in the sample chamber under its vapor pressure (~20 Torr at 25 °C) and allowed to adsorb to the solid surface. The cell was evacuated to 5 μm Hg and the temperature increased to 200 °C in order to remove all the hydrogen-bonded pyridine. The spectra were collected at 150 °C.

TPD−TGA Experiments. The density of strong Brønsted acid sites in aluminosilicate mesostructures was determined by temperature-programmed desorption of isopropylamine. The acid-catalyzed decomposition of amines has been used by several researchers to determine the density of Brønsted acid sites in zeolites.[13−16] This technique is based on the observation that amines react with acidic protons in order to form alkylammonium adsorption complexes, according to the scheme

$$HRNH_2 + Z\text{-}OH \rightarrow HRNH_3^+ + ZO^-$$

where Z is the zeolite surface.

These adsorption complexes undergo an acid-catalyzed cracking reaction at high temperatures:

$$HRNH_3^+ + ZO^- \rightarrow R + NH_3 + ZOH$$

In the case of isopropylamine adsorption, the adsorption complex is decomposed to propene and ammonia around 300 °C. If it is assumed that isopropylamine is chemisorbed on Brønsted acid sites with a stoichiometry of one isopropylamine molecule per acidic proton, the density of Brønsted acid sites can be determined by measuring the catalyst weight loss at 300 °C. This implicitly assumes that (i) the mobility of isopropylamine at low temperature is high enough for isopropylamine to saturate all the surface acid sites, and (ii) in materials with high acid site density, the chemisorption of an adsorbate molecule at one site does not prevent the adsorption of another molecule at a nearby acid site.

The temperature-programmed desorption of isopropylamine was carried out in a CAHN D200 microbalance with a sensitivity of 0.1 μg. The balance was connected to a vacuum line and could be evacuated to a base pressure of 10 mTorr using a diaphragm pump (MZ 2T from Balzers) connected to a molecular drag pump (TPD 020 from Balzers).

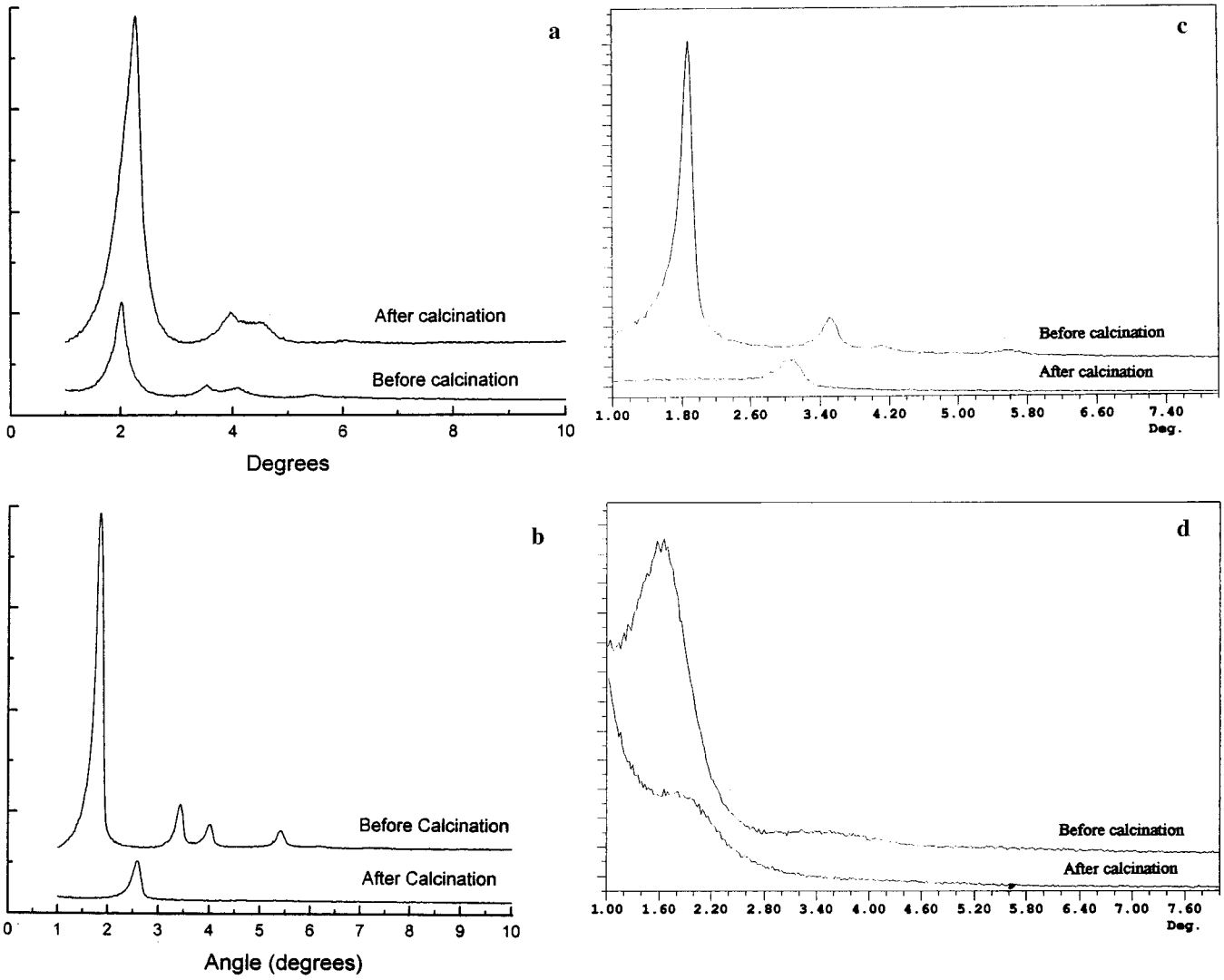

Figure 1. Powder X-ray diffractograms of (a) Si−MCM-41 and of the solids prepared with (b) Al hydroxide, (c) Al isopropoxide, and (d) Na aluminate.

Small amounts (10−30 mg) of sample were placed in a quartz sample pan. The sample was activated at 350 °C in a vacuum for 2 h (same activation temperature as for N_2 sorption), then cooled to 100 °C. The sample was exposed to isopropylamine (∼20 Torr) at 100 °C, until the sample weight became constant. The adsorption was completed at 100 °C in order to favor the diffusion of base throughout the channels. Then, the system was evacuated to 10 mTorr. Once the sample weight was constant, the oven temperature was raised from 100 to 400 °C with a heating ramp of 20 °C/min. Since diffusional effects are temperature-dependent, we repeated this experiment with different heating rates (5, 10, and 20 °C/min) for one sample. The shapes of the desorption curves were not functions of the heating rate. The weight loss of the samples at 300−350 °C varied by less than 10% among these experiments. From these results, we suggest that mass transport effects do not influence the shapes of these data. In a separate experiment, we examined the TPD spectrum of isopropylamine on zeolite H-Y ($SiO_2/Al_2O_3 = 10$) heated at 20 °C/min. This sample showed (not shown here) two distinct weight losses centered at 100−200 °C and above 300 °C. This TPD spectrum was very similar to that observed by Biaglow et al.[14] for acidic faujasite. These data on H-Y are included to show we are able to reproduce the literature for standard systems.

TABLE 1: Chemical Analyses

sample	synthesis pH	SiO_2/Al_2O_3, molar
Al mesostructures		
Al hydroxide	10.5	6.4
Al isopropoxide	12.5	4.6
Na aluminate	8.7	5.6
H-Y		2.75
AAA Alumina		6.2

Results

Chemical Analyses. The bulk SiO_2/Al_2O_3 ratios of the mesostructures are 6.4, 5.6, and 4.6 for the mesostructures prepared from Al hydroxide, Na aluminate, and Al isopropoxide, respectively, as determined by chemical analyses (Table 1). These values are close to the gel SiO_2/Al_2O_3 ratios ($SiO_2/Al_2O_3 \sim 5.2$).

Powder X-ray Diffraction. The powder X-ray diffractogram of the as-synthesized silica, which we call silica mesophase, shows four peaks at $2\theta = 2.0$, 3.6, 4.1, and 5.5° (Figure 1a). This X-ray diffraction pattern is similar to that reported by other researchers for MCM-41.[1,2,17] These peaks may be indexed on a hexagonal unit cell with $a = 2d_{100}/\sqrt{3} = 5.03$ nm. After sample calcination, the peaks were observed at $2\theta = 2.2°$, 3.8°, 4.7°, and 6.0° and the peak width at mid-height increased (Figure

TABLE 2: Powder X-ray Diffraction Results

sample	synthesis pH	unit cell size (nm) before/after calcination	unit cell contraction (%)
Si−MCM-41	12.7	5.03/4.45	12
Al−MCM-41			
Al hydroxide	12.6	4.95/3.50	29
	10.5	4.66/3.59	23
	8.1	4.54/2.99	34
Al isopropoxide	12.5	4.33/2.82	35
	8.7	5.43/3.36	28
	7.3	5.50/3.64	34

1a). The shifting of peak positions to higher angles indicates a lattice contraction of ∼11.5%. Chen et al. reported a 17.5% unit cell contraction in Si−MCM-41 upon calcination.[17] They indicated that, depending on synthesis conditions, the decrease in unit cell size could be as high as 25%. This lattice contraction is attributed to condensation reactions between adjacent silanol groups in the silica framework.

Typical powder X-ray diffractograms of the mesostructures prepared from Al hydroxide, Al isopropoxide, and Na aluminate are shown in Figure, 1 b, c, and d before and after calcination. The mesophases prepared from Al hydroxide show a four-peak diffraction pattern (Figure 1b) typical of MCM-41.[1,2,17] After calcination the powder X-ray diffractogram shows a single broad peak. For example, the powder X-ray diffractogram of the sample synthesized at pH 10.5 exhibits peaks at $2\theta = 1.8°$, 3.4°, 4.0°, and 5.4° before calcination and a single peak between 2.4° and 2.8° after calcination. No other peaks are observed in the 10°−50° range. It is not possible to attribute a one-peak diffraction pattern to a precise geometry; the structure could be either hexagonal, lamellar, or cubic. However, since the structure was hexagonal before calcination, it seems reasonable to believe that the structure is still hexagonal after calcination. The decrease in the number and in the sharpness of the peaks may have several origins: (i) the size of the diffracted domain decreased, and/or (ii) the strain in the crystal lattice increased, resulting in a material with shorter range order. The shift in peak location indicates a contraction of the unit cell ranging from 23% to 34% (Table 2). The change in unit cell size is therefore much larger than the 12% lattice contraction observed in the pure silica MCM-41.

The powder X-ray diffractograms of the mesophases prepared from Al isopropoxide also show a four-peak pattern, which may be indexed on a hexagonal unit cell (Figure 1c). For example, the solid synthesized at pH 8.7 shows peaks at $2\theta = 1.9°$, 3.6°, 4.1°, and 5.6°. The d_{200} and d_{210} reflection lines are weaker than in the X-ray diffractograms of the samples prepared from Al hydroxide (Figure 1b). After calcination, the PXRD shows a single-peak diffraction pattern ($2\theta = 3.0°$ for the solid synthesized at pH 8.7). Again, since the mesophase had a hexagonal symmetry before calcination, there are good reasons to believe that the calcined solids also have a hexagonal geometry. The unit cell contraction was much larger than in the parent Si−MCM-41 materials: ∼30% vs ∼12% (Table 2).

Finally, the powder X-ray diffractograms of the samples prepared from Na aluminate at pH 12.5 do not show any peaks, indicating that there are no periodicities in electron densities in these solids. When the synthesis pH was either 10.4 or 8.5, the mesophase powder X-ray diffractograms exhibit a broad peak at low angle ($2\theta = 1.6°$ for the mesophase prepared at pH 8.5) together with a broad shoulder between $2\theta = 2.8°$ and 4.6° (Figure 1d). Such XRD patterns have also been reported in the literature.[18,19,20] On the basis of data gained from transmission electron micrographs (TEM) and electron diffraction patterns, Tanev et al. established that these solids had a hexagonal geometry.[18] They attributed the diffuse scattering at ∼5° to the finite size of the scattering domain. Considering the fact that the solids prepared from Al hydroxide and Al isopropoxide have a hexagonal symmetry, there are some reasons to believe that the solids prepared from Na aluminate also have an hexagonal geometry. The XRD of the calcined mesophases shows a broad shoulder around $2\theta = 2°$ which indicates a periodicity in electron density within the solid. Other diffraction techniques should be used in order to identify the solid symmetry.

N_2 Sorption. The N_2 adsorption isotherms of the calcined mesostructures are shown in Figure 2. Their physical characteristics are listed in Table 3.

The N_2 sorption isotherm of the pure silica mesostructure is characterized by an adsorption step at relative pressure P/P_0 near 0.35 due to capillary condensation in mesopores (Figure 2a). This is a type IV isotherm typical of MCM-41 mesostructures.[21] The mesopore volume is 0.93 cm^3/g and the average pore diameter is 3.4 nm with an average wall thickness of 1 nm (Table 3).

The nitrogen adsorption isotherms of the solids prepared from Al hydroxide (Figure 2b**)** show an enhanced nitrogen uptake at relative pressures between 0.1 and 0.15, indicative of a population of uniformly sized pores. The average pore diameter is 2.2 nm, as estimated using the density functional theory to develop the pore size distribution. The average pore diameter is independent of the pH of synthesis. The mesopore volume (between 0.43 and 0.59 cm^3/g solid) is lower in the aluminosilicate mesostructures than in the pure silica MCM-41 (0.93 cm^3/g solid) and depends on the pH of synthesis. For example, solids prepared at pH ∼ 10.5 have a porous volume of 0.59 cm^3/g in contrast to 0.50 and 0.43 cm^3/g for solids prepared at pH 12.6 and 8.1, respectively (Table 3).

The adsorption isotherms of the solids prepared from Na aluminate are type IV isotherms, characterized by an enhanced adsorption at relative pressures between 0.2 and 0.3 (Figure 2c). The pore diameter was 3.2, 2.9, and 2.7 nm for solids prepared at pH 12.5, 10.4, and 8.5 respectively, as estimated from density functional theory (Table 3). The mesopore volume increased when the alkalinity of the synthesis mixture decreased: it was 0.30 cm^3/g for solids prepared at pH of 8.5 and 10.4, versus 0.23 cm^3/g for solids prepared at pH 12.5. The mesopore volume was therefore lower than in the materials prepared from Al hydroxide. The slope of the adsorption isotherm at relative pressures between 0.4 and 0.8 is larger in solids prepared from Na aluminate than in solids prepared from Al hydroxide. Nitrogen uptake in this range of pressures is due to the multilayer coverage of the external surface of the crystals. This indicates that the particle size and particle aggregation is probably different in these two families of solids (vide infra). The amount of nitrogen adsorbed on the external surface of the crystals prepared from Na aluminate is probably nonnegligible in comparison to the amount of nitrogen condensed in mesopores, and we overestimate the mesopore volume when we calculate it from the nitrogen uptake at $P/P_0 = 0.5$. The adsorption isotherm of the solids prepared at pH 8.5 undergoes a sharp increase in nitrogen uptake at high pressure ($P/P_0 > 0.9$), indicative of a significant amount of interparticle mesoporosity.

Finally, the nitrogen adsorption isotherms of the solids prepared from Al isopropoxide are of type I (Figure 2d). The absence of a sharp step at low pressure ($P/P_0 < 0.1$) indicates that these solids have a wide distribution of micropore sizes, as confirmed by the DFT pore size distribution. Therefore, these solids do not have any interesting pore size selectivity.

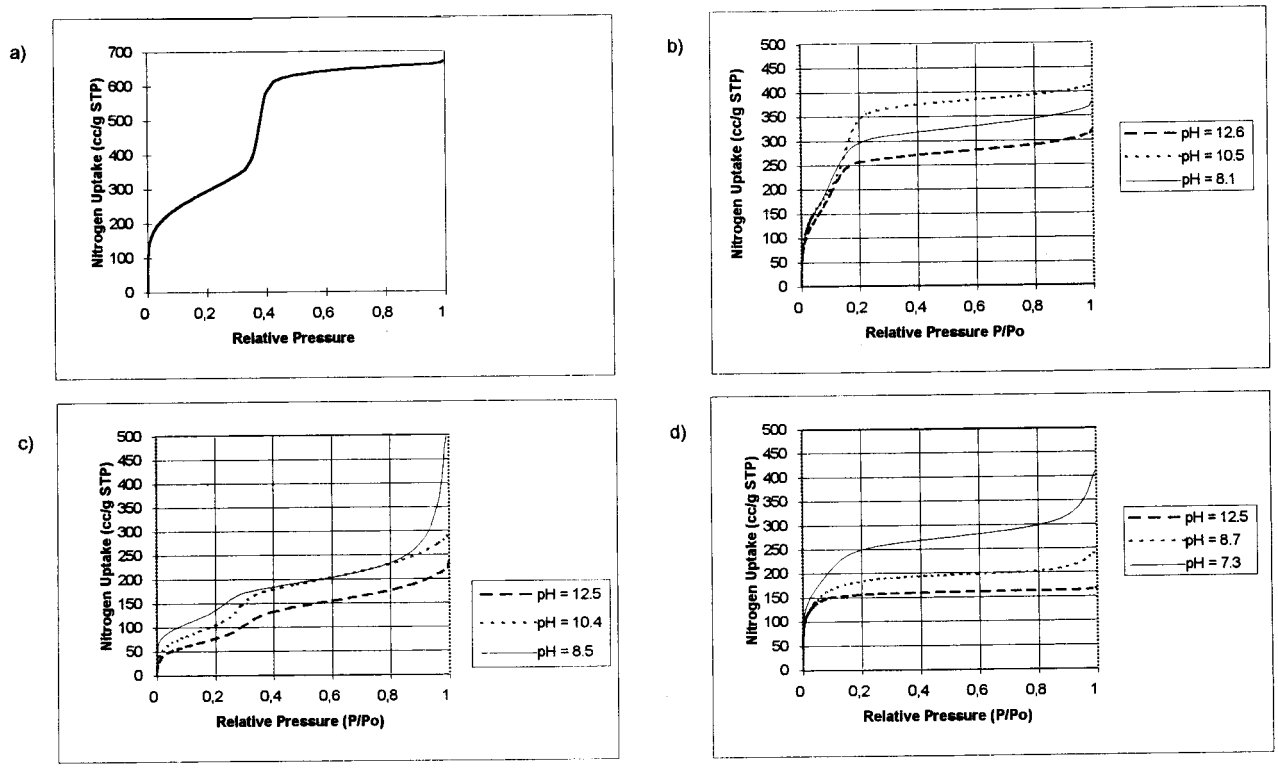

Figure 2. Nitrogen adsorption isotherms of (a) Si-MCM-41, and aluminosilicate structures prepared with (b) Al hydroxide, (c) Na aluminate, and d) Al isopropoxide.

TABLE 3: Porosity Data

sample	synthesis pH	mesopore vol (cm^3/g)	DFT av pore dia (nm)	wall thickness[a] (nm)
Si−MCM-41	12.7	0.93	3.4	1.0
Al/Si−MCM-41				
Al hydroxide	12.6	0.43	2.2	1.3
	10.5	0.59	2.2	1.39
	8.1	0.50	2.2	0.79
Al isopropoxide	12.5	0.26	0.5−2.0	
	8.7	0.30	0.5−2.0	
	7.3	0.42	0.5−2.0	
Na aluminate	12.5	0.22	3.2	b
	10.4	0.30	2.9	b
	8.5	0.30	2.7	b
AAA Alumina		0.77	2.5−12.0	
HY		0.36	0.8	

[a] Wall thickness = unit cell size after calcination − DFT average pore diameter. [b] The wall thickness was not calculated for these solids because the unit cell size cannot be determined without ambiguity.

Scanning Electron Microscopy. Samples prepared with Al-$(OH)_3$ appear as aggregates of smooth platelets, 1−2 μm in diameter (Figure 3a). Although most platelets are irregular in shape, we were surprised to observe that some platelets show clearly cut edges that intersect at angles close to 120°. This geometry is consistent with the hexagonal crystal structure. Some amorphous material is also observed that may be unreacted gel. The morphology of the solid did not change after calcination.

As expected from sorption measurements, the morphology of the samples prepared with Na aluminate is strikingly different. The SEM micrograph in Figure 3b shows dense aggregates of very small primary particles (ca. 100 nm) which should give rise to macroporosity. The morphology of the samples did not change upon calcination.

^{27}Al MAS NMR. We show in Figure 4 the ^{27}Al MAS NMR spectra of the solids developed from Al hydroxide, Na aluminate, and Al isopropoxide, as these spectra are characteristic of all the samples. The ^{27}Al MAS NMR spectra of the uncalcined mesostructures (left-hand side) exhibit a single peak at 55 ppm, irrespective of the Al source. In zeolites, a peak near 55 ppm is usually attributed to tetrahedral Al. We conclude that all the Al present in the mesophases is in tetrahedral environment. Therefore, it seems that the Al source does not have much influence on the Al environment in the as-synthesized mesostructure.

After calcination, the spectra of the mesostructures exhibit a new signal near 0 ppm, attributed to octahedral Al (Figure 4, right-hand side). A closer inspection of Figures 4, a and b, indicates that an additional peak could exist near 25−30 ppm. This peak is definitely present in the spectrum of the mesostructure prepared from Al isopropoxide (Figure 4c). Such a peak was detected by Ray et al. who used double rotation and variable field Al NMR spectroscopy to study Al environment in steamed HY faujasites.[22] The authors proposed that the peak near 30 ppm corresponds to either a nonframework tetrahedral Al species in a highly distorted environment or a pentacoordinate species. Since we did not have access to variable field or DOR techniques, we were not able to identify the origin of the shoulder near 25−30 ppm. We conclude that the calcination treatment and the template removal have a profound effect on the Al environment. A fraction of Al changes environment and, possibly, acquires a new symmetry. We detected three kinds of Al environments in the mesostructures: tetrahedral Al, octahedral Al, and a third type of Al environment, which we were not able to identify. Therefore, we did not attempt to quantify the proportion of tetrahedral to octahedral Al in the calcined mesostructures.

^{29}Si MAS NMR. One sample having a SiO_2/Al_2O_3 ratio 5.6 was examined by ^{29}Si MAS NMR. This sample showed a single, broad resonance with a peak maximum at −94.22 ppm. Two standards were examined for the same machine settings:

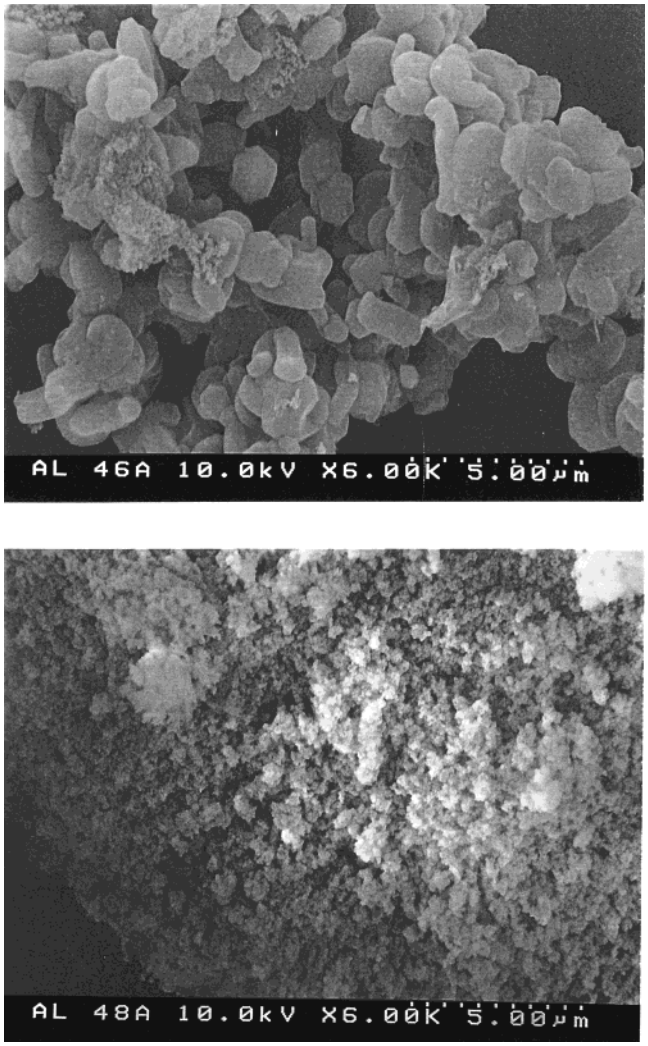

Figure 3. Scanning electron micrographs of the as-synthesized solids prepared from (a, top) Al hydroxide and (b, bottom) Na aluminate.

HZSM-5 with a SiO_2/Al_2O_3 ratio 37.5) and a HY faujasite having a SiO_2/Al_2O_3 ratio 3. These standards showed peaks at −113 ppm for the HZSM-5 and four peaks for the HY faujasite at the following positions: −89, −95, −103, and −108 ppm. These results suggest that the Si environments in aluminosilicate mesostructures and in zeolites are different. The diffuse nature of the Si NMR pattern suggests that the silicon environment in mesostructures is not unlike that in glassy solids.

Infrared Spectroscopy. Figure 5 shows typical infrared spectra of aluminosilicate mesostructures chemisorbed with pyridine. All the spectra show infrared absorption bands near 1545 and 1454 cm^{-1}. In zeolites, these absorption bands are typically attributed to pyridine protonated by Brønsted acid sites and to pyridine coordinated to Lewis acid sites, respectively. The band near 1490 cm^{-1} corresponds to vibration modes of pyridine bound to both Brønsted and Lewis acid sites. Therefore, this band may not be used to discriminate between Brønsted and Lewis acid sites. In order to compare the acid site distribution of the mesostructures with that of known aluminosilicate catalysts, the spectra of acidic faujasite and an amorphous aluminosilicate matrix (AAA Alumina) have been added to Figure 5. Both these solids are used as fluid cracking catalysts (FCC) in industry. AAA Alumina resembles the mesostructures in terms of local atomic arrangement but it possesses a wide distribution of mesopore sizes.[23]

Aluminosilicate mesostructures, AAA Alumina, and acidic faujasite all show IR spectra that are consistent with solids having Brønsted and Lewis acid sites (Figure 5). The ratio of peak areas was used to estimate the relative populations of acidic sites in the catalysts. The reliability of this technique rests on knowing that the extinction coefficients for the chemisorbed species is similar and constant between experiments. The ratio of Brønsted to Lewis acid site density is similar in aluminosilicate mesostructures and AAA Alumina. It is much lower than in acidic faujasite. In agreement with other reports,[24] the −OH stretching region of aluminosilicate mesostructures and AAA Alumina present a single band around 3742 cm^{-1} (not shown). In contrast, the −OH stretching region of acidic faujasite presents several bands between 3800 and 3500 cm^{-1}, indicating the presence of different types of surface −OH groups.

TPD-TGA Measurements. Figure 6 is a typical TPD profile of aluminosilicate mesostructures saturated with isopropylamine. When the oven temperature was raised from 100 to 300 °C (time interval between 0 and 10 min), the mesostructure weight decreased steadily. The rate of weight loss increased in the 300−350 °C range (time interval of 10−13 min) and tailed off once the oven temperature reached 350 °C (time = 15 min). In contrast to this result, the TPD spectrum of the standard, H-Y zeolite ($SiO_2-Al_2O_3 = 10$) showed two distinct weight losses: a first loss between 100 and 200 °C which we attribute to the desorption of weakly adsorbed isopropylamine, and a second weight loss above 300 °C owing to the decomposition of isopropylamine to propene and ammonia. This TPD profile in Figure 6 for the mesoporous material is very similar to the TPD profile reported by Biaglow et al.[14] for acidic faujasite. These authors showed that the very broad desorption feature below 300 °C corresponded to unreacted isopropylamine desorption, as analyzed by mass spectrometry. Propene and ammonia evolved simultaneously between 300 and 375 °C, owing to isopropylamine decomposition on Brønsted acid sites. The shape of the TPD profile in Figure 6 may have several origins: (i) diffusional effects in the desorption process skews the kinetics of desorption, and (ii) the existence of strong adsorption sites that are not Bronsted acid sites. The data we provided for varying the heating rate suggests that mass transport effects cannot explain the shapes of the desorption curves. The data of pyridine IR does show the existence of Lewis acid sites. It has been shown by microcalorimetry that the heat of adsorption of ammonia in aluminosilicate mesostructures ($SiO_2/Al_2O_3 = 64$ to 8) decreased monotonically with increasing surface coverage of the ammonia adsorbate.[9] The existence of Lewis acid sites inside the channels or at the external surfaces of the crystals may decrease the mobility of the chemical species and slow the desorption of the species. This decreased desorption may explain the TPD profile in Figure 6.

The weight loss attributed to isopropylamine cracking on Brønsted acid sites was measured, and the density of Brønsted acid sites was calculated for each catalyst. The main assumptions were (i) all the products of isopropylamine cracking left the solid in the 290−320 °C temperature range, (ii) each isopropylamine molecule was protonated on exactly one Brønsted acid site, and (iii) each Brønsted acid site was associated with exactly one four-coordinated Al. The results are listed in Table 4.

The surface Brønsted acid site density of the mesostructures prepared from Al hydroxide is 0.35 μmol H^+/m^2. The TPD profiles of the mesostructures prepared from Na aluminate in their Na^+ form do not show any indication of isopropylamine cracking, indicating that there are no Bronstedt acid sites active

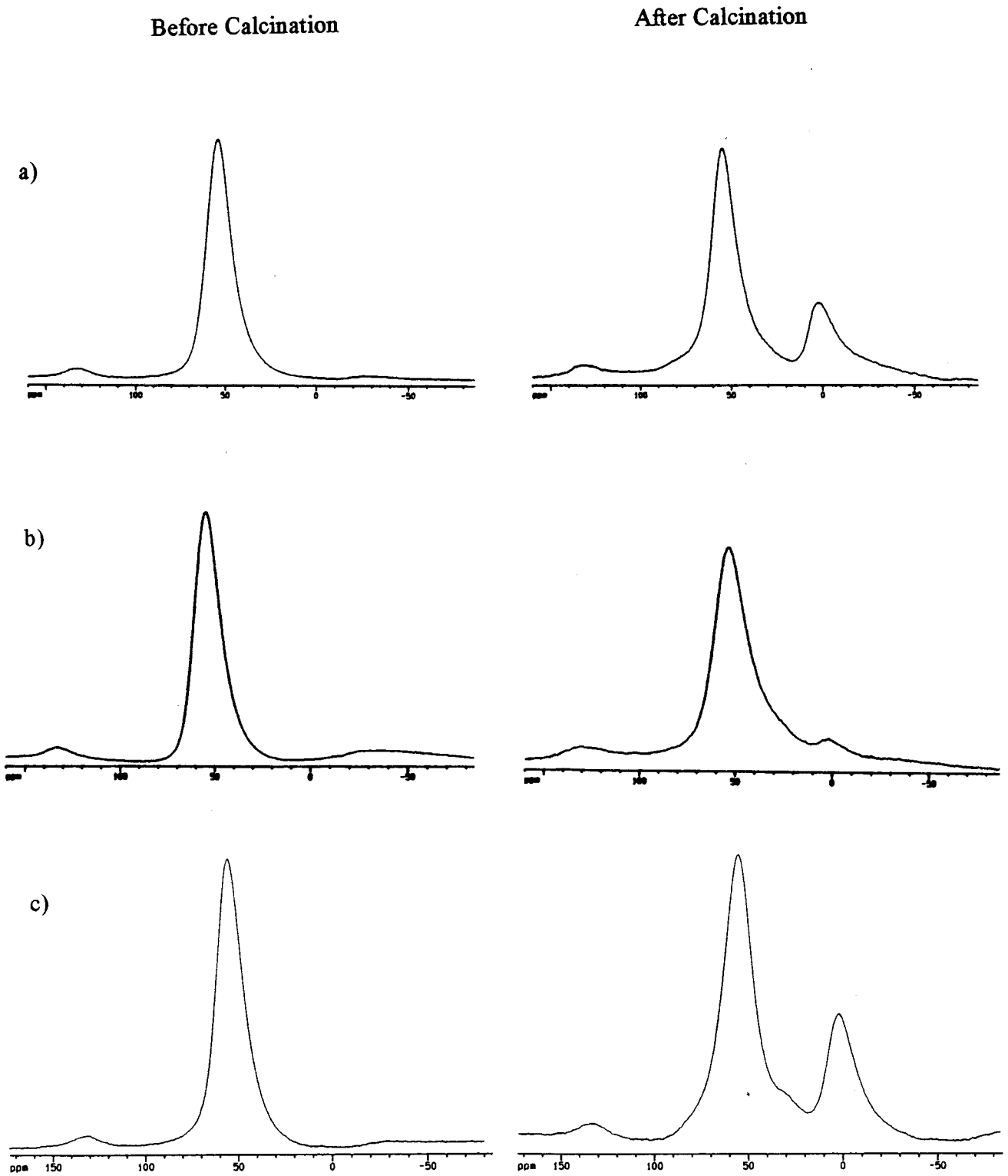

Figure 4. ^{27}Al MAS NMR spectra of the materials prepared from (a) Al hydroxide, (b) Na aluminate, and (c) Al isopropoxide before and after calcination.

for this reaction on either the external or internal surface of the solid. In contrast, the surface Brønsted acid site density of the mesostructures after ammonium exchange and calcination is around 0.36 μmol H^+/m^2. Assuming that each Brønsted acid site active for isopropylamine cracking was created by the presence of Al(III) ions in tetrahedral coordination, we calculated an "effective" SiO_2/Al_2O_3 ratio (Table 4). In both aluminosilicate mesostructures, the effective SiO_2/Al_2O_3 ratio is much larger than the bulk SiO_2/Al_2O_3 ratio: it is 42 in mesostructures prepared with Na aluminate and 23 in mesostructures prepared with Al hydroxide. Therefore, a large fraction of the Al in the sample does not yield any Brønsted acid sites active for isopropylamine cracking reaction. Some of the Al may be present as extraframework Al that gives Lewis acid sites and some of it may be embedded in the walls of the mesostructures (close to 1.5 nm thick) and, therefore, be inaccessible to reactants.

The surface Brønsted acid site density of the mesostructures and AAA Alumina are very similar, 0.36 μmol H^+/m^2. In qualitative agreement with IR results, the Brønsted acid site

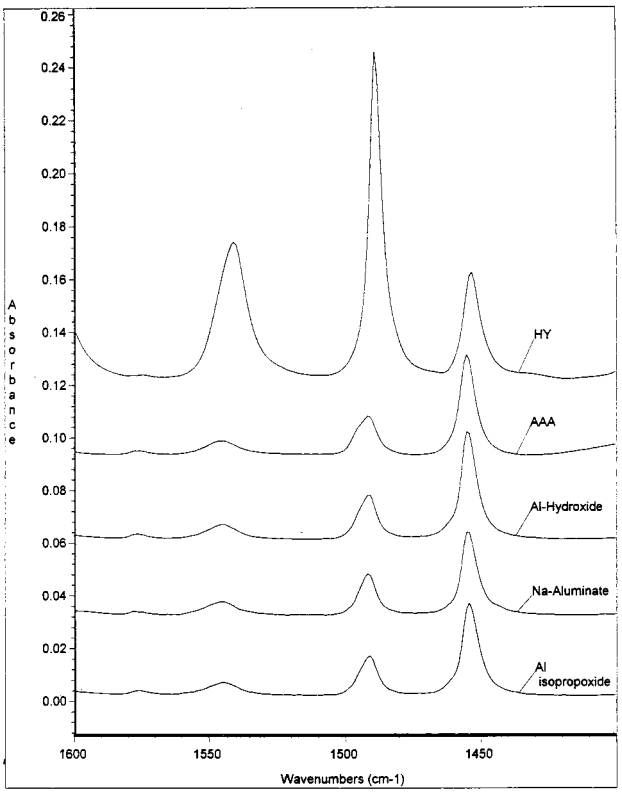

Figure 5.

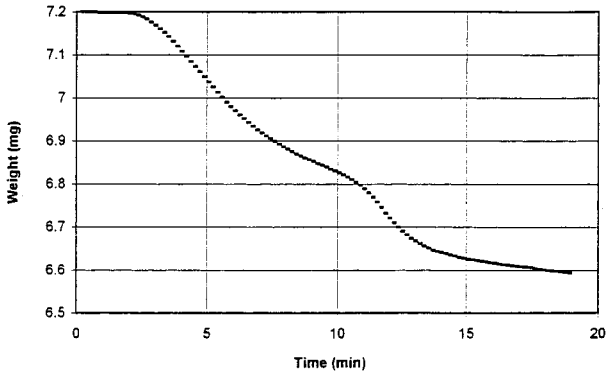

Figure 6. Typical TPD−TGA profile of aluminosilicate mesostructures (heating rate: 20 °C/min).

TABLE 4: Brønsted Acid Site Density in Aluminosilicate Mesostructures

Al source	synthesis pH	Brønsted acid site density μmol H^+/g	Brønsted acid site density μmol H^+/m^2	effective SiO_2/Al_2O_3
Al hydroxide	10.5	370	0.35	23
Na aluminate	8.5			
Na form		a	a	
H^+ form		200	0.36	42
zeolite HY[b]		848		9.8
AAA		172	0.357	48.3

[a] No indication of Brønsted acid sites. [b] The sample looked gray after analysis, indicating that a significant amount of coke had formed.

density is much lower in aluminosilicate mesostructures and AAA Alumina than in acidic faujasite. On a weight basis, it is 848 μmol H^+/g for acidic faujasite vs 370 μmol H^+/g and 200 μmol H^+/g in mesostructures prepared with Al hydroxide and Na aluminate, respectively. It is believed that a high fraction of the Al incorporated in the mesostructure is embedded in the walls and, therefore, is not accessible to reactant molecules.

Discussion

Several authors have documented the effect of inorganic precursors upon the structure and the properties of MCM-41 mesostructures. For example, Chen et al. showed that sodium silicate reacted faster than fumed silica to form the MCM-41 mesophase, as documented by the PXRD of the mesophase at different reaction times.[17,25] Luan et al. conducted an extensive study of the influence of the Al precursor and Al content on the structure and properties of Al−MCM-41.[3,4] In the present case, we examined the effect of Al precursors on the structure and properties of mesostructures prepared from gels with $SiO_2/Al_2O_3 = 5$. We chose three Al precursors: Al hydroxide, Na aluminate, and Al isopropoxide. The Si precursor was tetraethyl orthosilicate, $Si(OC_2H_5)_4$. It is of interest to determine if and how the relative rates of aluminate and silicate anion formation influence the composition and the structure of the resulting solids.

Two of the Al sources, Na aluminate and Al hydroxide, form directly the anion by dissolution in the aqueous base, tetraethylammonium hydroxide, according to the following schemes:

$$NaAlO_2 \cdot xH_2O \xrightarrow{H_2O,\ OH^-} Na^+[Al(OH)_4]^- \quad (1)$$

$$AlOH_3 \cdot xH_2O \xrightarrow{H_2O,\ TEA^+OH^-} TEA^+[Al(OH)_4]^- \quad (2)$$

The Al isopropoxide first undergoes a series of hydrolysis reactions:

$$Al(OC_3H_7)_3 + xH_2O \xrightarrow{H_2O,\ OH^-} Al(OC_3H_7)_{3-x}(OH)_x + xC_3H_7OH \quad (3)$$

If the hydrolysis is not complete, then we expect to see several Al species in equilibrium: $Al(OC_3H_7)_{3-x}(OH)_x$, where $x \leq 3$. The ultimate product of reaction 3 is $Al(OH)_3$, which gives the $[Al(OH)_4]^-$ anion according to eq 2. Thus, the rate of formation of Al anions may be slower from the alkoxide precursor than from Al hydroxide or Na aluminate. In addition, it releases a large amount of propanol in the reaction mixture.

In order to favor the complete hydrolysis of Al isopropoxide, the Al source was first dissolved in the organic base. This solution was slowly added to tetraethyl orthosilicate, together with the surfactant. Tetraethyl orthosilicate is not soluble in aqueous solution. Its hydrolysis is base-catalyzed and proceeds according to the following scheme:

$$Si(OC_2H_5)_4 + xH_2O \xrightarrow{H_2O,\ OH^-} Si(OC_2H_5)_{4-x}(OH)_x + xC_2H_5OH \quad (4)$$

The ethanol released as a byproduct is sufficient to homogenize the synthesis mixture. Within 3−4 min, the synthesis mixture turned from a yellow transparent solution to a white milklike gel. The pH of the synthesis mixture was slowly decreased with the addition of HCl. The mixture was then slightly heated in order to vaporize the alcohol formed as a byproduct of alkoxide hydrolysis (reactions 3 and 4).

We believe that the mesophase assembly proceeds according to a mechanism similar to that proposed by Chen et al.[25] and Huo et al.[26,27] for pure silica MCM-41. Charged Si and Al species formed by reactions 1−4 compete to displace the surfactant counteranions (chloride or hydroxide ions), as shown in Figure 7. Here the surfactant counteranions, Cl^-, are replaced with Si-bearing anions or Al-bearing anions. A priori, the

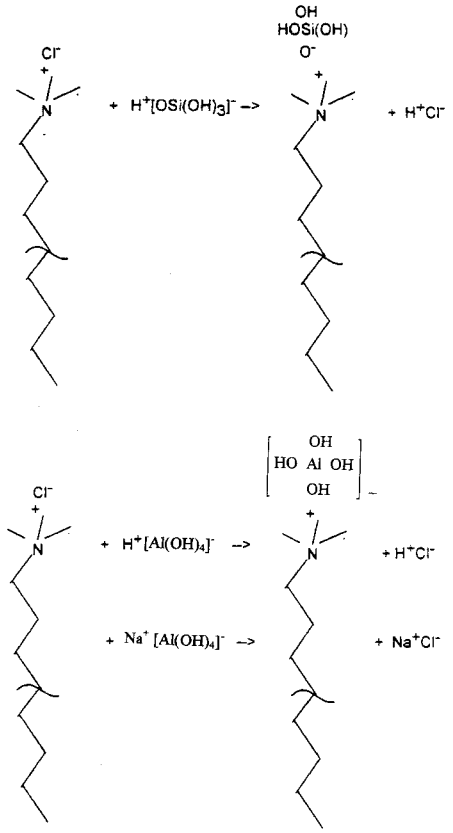

Figure 7. Schematic of ion exchange at cetyltrimethylammonium cation.

surfactant molecules may originate from single solution species as well as from spherical or cylindrical micelles. The Si-bearing anions are generated by the hydrolysis of tetraethyl orthosilicate (TEOS). Thus, in the early parts of the synthesis, the concentration of Al-bearing anions (e.g., $Al(OH)_4^-$) at the surfactant head should be greater than the concentration of silicate species. For this reason, we expect the surfactant/inorganic interface to be enriched in Al species. We speculate that the ion-exchange reaction ($Al(OH)_4^-$ for Cl^-) occurs very rapidly. The synthesis system behaves as a conventional liquid crystal in which inorganic species are attached to the surfactants. This system acquires its minimum energy by changing configuration. The inorganics-coated micelles grow in length. Simultaneously, the condensation of inorganic species at the micelle surface drives the formation and the stabilization of hexagonal close-packed arrays of aluminosilicate coated micelles, typical of the MCM-41 mesophase. Inorganics condensation is favored by the thermal treatment at 110 °C, which stabilizes the hexagonal mesophase. The condensation of adjacent inorganic species is described in Figure 8. We show here the initial arrangement of aluminate and silicate anions at the surfactant head. This particular arrangement was developed assuming that there were no adjacent Al ions. Complete condensation of the aluminosilicate species is not possible since anions are necessary for charge compensation of the surfactant cations. Furthermore, we notice that bulky charge-compensating sodium cations may frustrate the framework condensation.

According to this simple model, the bulk SiO_2/Al_2O_3 ratio in the resulting mesophase should be similar to the SiO_2/Al_2O_3 ratio in the starting gel. Indeed, the chemical analyses in Table 1 show that the bulk SiO_2/Al_2O_3 ratio were 6.4, 5.6, and 4.6 in the solids prepared from Al hydroxide, Na aluminate, and Al isopropoxide, respectively. These values are close to the 5.2 SiO_2/Al_2O_3 ratio in the synthesis gel. The powder X-ray diffractogram patterns for the mesophases prepared from Al hydroxide and aluminum isopropoxide show four reflection lines that may be indexed on a hexagonal unit cell. These X-ray diffractogram patterns are similar to PXRD patterns reported by other investigators for silica-MCM-41.[1,2,17] It is accepted that these reflection lines stem from the hexagonal close-packed arrangement of the inorganic tubes. However, the solids prepared from sodium aluminate do not demonstrate the same degree of

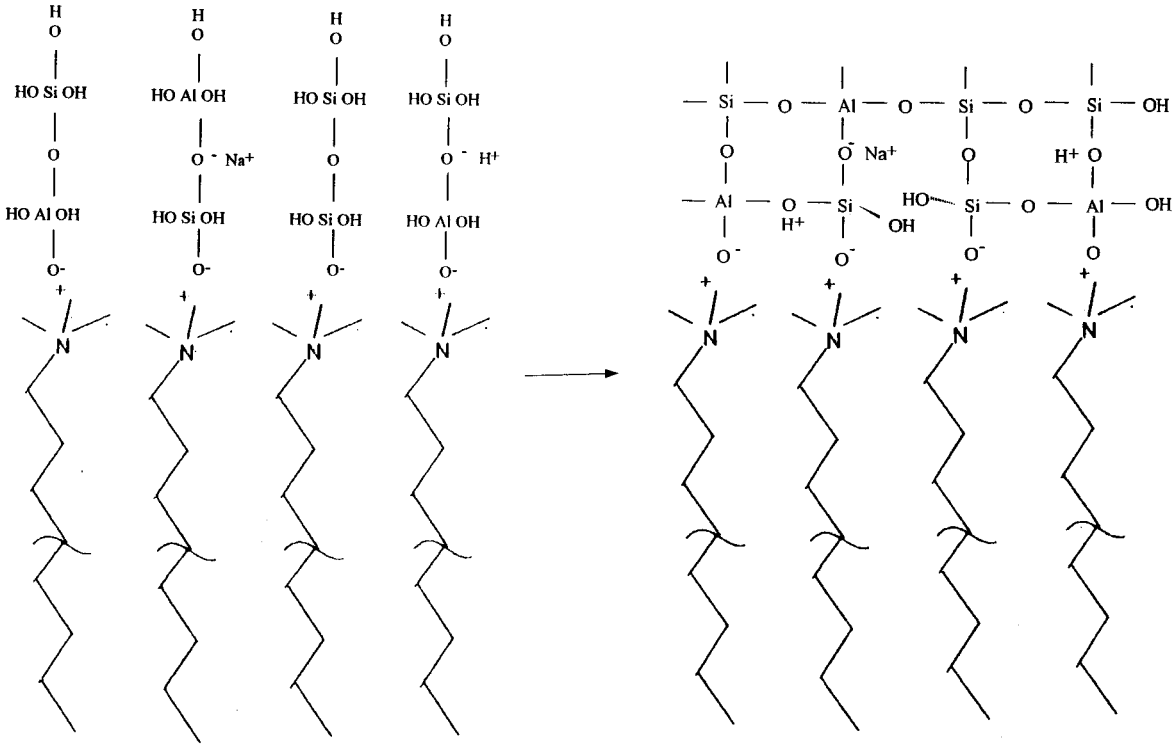

Figure 8. Schematic of self-assembly and condensation reactions.

order, since their PXRD only exhibit a broad peak around $2\theta = 2°$ and a broad shoulder between 3° and 5°. We suggest that sodium ions residing on the surface of the inorganics-coated micelles in the vicinity of Al ions frustrate the hexagonal close-packed arrangement of the tubes, thus resulting in more disorder at the length scale corresponding to that of the tube diameter. Although protons may also reside in the same position, they do not interfere with the packing of the inorganic tubes because of their small size.

The mesophases prepared from Al isopropoxide show a marked increase in unit cell size (4.3 to 5.5 nm) for decreasing the gel solution pH from 12.5 to 7.3 (Table 2). The solubility of silica species is known to decrease when the solution pH decreases from 12 to 7.[28,29] Therefore, it is believed that, at low pH, the equilibrium between single silicate solution species and precipitated silica is displaced toward silica precipitation around the surfactant micelles. This favors the formation of thicker walls and larger unit cells. This is in qualitative agreement with the work of Coustel,[30] who noticed that mesostructures with thicker walls were prepared when the OH^-:SiO_2 ratio in the synthesis gel of Si−MCM-41 decreased.

The four-peak diffraction patterns of the mesostructures prepared from Al hydroxide and Al isopropoxide were transformed into a one-peak diffraction pattern after calcination. This indicates a considerable loss of order in the solids upon template removal. Simultaneously, the frameworks underwent a major contraction: for example, the unit cell contraction was between 23% and 35% in aluminosilicate mesostructures, compared to only 12% in the pure silica mesostructure (Table 2). We can push the comparison even further if we recall that reported unit cell contractions for cubic and hexagonal faujasite did not exceed 1% upon template removal.[17] It is believed that the incorporation of large amounts of Al in the synthesis gel of Si−MCM-41 limits the condensation of the inorganic walls. The walls of as-synthesized mesophases may contain voids. They may also contain encapsulated water molecules produced by inorganic condensation as well as sodium cation in the vicinity of Al species (Figure 8). As a result, the synthesis products afford poorly cross-linked walls subjected to high internal strains. The walls are severely damaged by the high-temperature treatment (600 °C) used to remove the organic template. The entire framework contracts, and fractions of the mesopores collapse, yielding a mesopore volume far lower than the mesopore volume of Si−MCM-41 (0.59 and 0.30 cm^3/g in mesostructures prepared from $Al(OH)_3$ and Na aluminate compared to 0.93 cm^3/g in Si−MCM-41) as well as mesopores smaller than in Si−MCM-41: 2.2 and 2.7 nm diameter for mesostructures prepared from Al hydroxide and Na aluminate, vs 3.4 nm in Si−MCM-41 (Table 3). Therefore, even though they are prepared from the same surfactant, cetyltrimethylammonium species, the mesostructures prepared from Al hydroxide and sodium aluminate exhibit different average pore diameters. The absence of Brønsted acid sites in the Na^+ form of the mesostructures (as documented by TPD of isopropylamine) indicates that the negative charges created by Al in tetrahedral coordination are compensated by sodium ions in the surface region. It is believed that the presence of Na ions at the surfactant/inorganic interface modifies the wall curvature. Therefore, the mesostructures formed upon calcination afford larger pores than the solids prepared from Al hydroxide (Table 3).

When Al isopropoxide was used as Al precursor, the final materials possessed a distribution of pore sizes much wider than expected: between 0.5 and 2.0 nm diameter. The hydrolysis of Al isopropoxide proceeds according to reaction 3. It releases a large amount of propanol in solution, in addition to the ethanol produced by the hydrolysis of tetraethyl orthosilicate ($Si(OC_2H_5)_4$). The presence of excess alcohol has been shown to disrupt the formation of liquid crystal phases in C_{16}TMA-containing solution[31] and to prevent the formation of MCM-41 mesophases.[32] The mesophases prepared from Al isopropoxide all have a four-peak diffraction pattern (Figure 1c), typical of MCM-41, indicating that the excess alcohol did not hinder the long-range hexagonal packing of the micelles. We believe that the excess alcohol limits the inorganic condensation. The mesophases thus formed were not stable to the calcination treatment used to remove the template, resulting in solids with a wide distribution of pore sizes.

The NMR measurements describe the environment of the Si and Al atoms throughout the solid. It is clear that the ^{29}Si NMR data do not permit a clear picture of the silicon environment. The silicons reside in a variety of environments. However, the ^{27}Al NMR data do permit some knowledge regarding the Al local environment. The as-synthesized solids, so-called mesophases, all show aluminum in tetrahedral environment regardless of the precursor (signal at 55 ppm, Figure 4). However, when the solids are calcined, all the spectra show the presence of octahedral Al ions (signal at 0 ppm). In addition, some Al ions reside in a third type of environment which we were not able to identify (signal around 25−30 ppm): Ray et al. suggested that this signal corresponds to pentacoordinated Al or tetrahedral Al in a highly distorted coordination sphere.[22] These data suggest that, following the calcination process and the template removal, the Al environment in the walls was modified. Some of the Al acquired a new symmetry. This new symmetry perhaps required the Al ions to segregate from the inorganic framework. These Al ions may be located inside the channels or on the outer surface of the crystals. A fraction of Al ions, however, stayed in tetrahedral coordination. We believe that these Al species are embedded in the silicon oxide matrix, in substitution position for Si atoms. The framework negative charges introduced by the tetrahedrally coordinated Al are compensated by either protons or sodium cations. When the charge-compensating protons are in the surface region, they create Brønsted acid sites accessible for reactant species.

We used the temperature-programmed desorption of isopropylamine in order to quantify the density of accessible Brønsted acid sites in the aluminosilicate mesostructures. The density of Brønsted acid site (on a weight basis) was lower in aluminosilicate mesostructures than in acid faujasite, 370 μmol H^+/g in Al−MCM-41 prepared from Al hydroxide vs 848 μmol H^+/g in acidic faujasite (Table 4). However, at comparable SiO_2/Al_2O_3 ratios, the surface Brønsted acid site densities in aluminosilicate mesostructures and in an amorphous alumina silica matrix were similar, 0.35 μmol/m^2 (Table 4). These results suggest that the surface of Al−MCM-41 is comparable to the surface of amorphous aluminosilicates. Assuming that each Brønsted acid site active for isopropylamine cracking was created by the presence of Al(III) ions in tetrahedral coordination, we calculated an "effective" SiO_2/Al_2O_3 ratio. The effective SiO_2/Al_2O_3 ratio was 42 in the mesostructures prepared with Na aluminate and 23 in mesostructures prepared with Al hydroxide. It was therefore much larger their bulk SiO_2/Al_2O_3 ratios of 5.6 and 6.4, respectively. Therefore, a large fraction of the Al in the mesostructure does not yield any active Brønsted acid sites.

Both X-ray and ^{27}Al NMR analyses indicate that the calcination treatment and the removal of the template transformed the wall structure. Prior to calcination, the mesophases all show Al in tetrahedral environment, regardless of the Al

source (Figure 4). After calcination, we detected three kinds of Al environments in the mesostructures. Unfortunately, NMR spectroscopy does not yield any information about Al location and distribution within the mesostructure. We propose that, upon calcination and without the restraining influence of the template, some Al ions acquired a new symmetry, which required them to segregate from the framework. These Al ions may be located inside the mesopores or outside the mesoporous domains. They are responsible for the Lewis acid sites detected by infrared spectroscopy and by temperature-programmed desorption of isopropylamine. Edler et al. proposed that the walls of silica MCM-41 were made from silica layers of different density:[33] high-density silica where silica-encapsulated micelles interconnect to form the hexagonal phase during synthesis, and low-density silica at the micelle surface. We propose that the wall structure of Al−MCM-41 is not uniform either. For example, different Al environments may be created inside the walls as a result of the thermal treatment and the removal of the template. We propose that the coordination sphere of some Al residing in the walls is distorted by the calcination treatment. These ions are responsible for the NMR signal near 25−30 ppm. The NMR signal near 55 ppm corresponds to Al ions in tetrahedral environment. These Al ions are in substitution positions for Si atoms and introduce local negative charges in the framework, compensated by either protons or sodium cations. When the charge-compensating cations are protons located in the surface region, they create Brønsted acid sites accessible to reactants. Therefore, only a fraction of the Al introduced in the structure yields active Brønsted acid sites and the effective SiO_2/Al_2O_3 is much higher than the bulk SiO_2/Al_2O_3 ratio, as calculated from temperature-programmed desorption of isopropylamine. Further work should focus on improving the condensation of the walls in the mesophase and finding a milder way to remove the template in order to limit the damage induced in the walls by the calcination treatment and improve the mesostructure effective SiO_2/Al_2O_3 ratio.

Conclusion

Mesoporous aluminosilicate mesostructures with a $SiO_2/Al_2O_3 \sim 5$ have been synthesized by direct incorporation of Al in the synthesis gel. The morphology, structure, and porosity of the mesostructures varied with the Al source and the pH of synthesis. In general, Al incorporation led to a major decrease in mesopore volume and average pore diameter, when compared to the same properties in silicon-MCM-41. For example, the mesostructures prepared from Al hydroxide at pH 10.5 showed an average pore diameter of 2.2 nm and a mesopore volume of 0.59 cm^3/g, compared to 3.4 nm average pore diameter and 0.93 cm^3/g mesopore volume for the pure silica MCM-41 parent material.

The aluminosilicate mesostructures had a surface Brønsted acid site density similar to the surface Brønsted acid site density of an amorphous aluminosilica matrix. However, the Brønsted acid site density of the aluminosilicate mesostructures (on a weight basis) was much lower than in acidic faujasite. It is believed that the mesostructures contain domains of amorphous alumina that yield Lewis acid sites of variable strength. In addition, a large fraction of the four-coordinated Al atoms inserted in the framework are embedded in the walls (about 1.5 nm thick). Since these Al sites are not in the surface region, their charge-compensating protons do not contribute to the surface acidity of the mesostructure.

Acknowledgment. The authors thank the Trevira Corp. (Spartanburg, SC) for the support of parts of this project. We also acknowledge the School of Mechanical Engineering, Georgia Institute of Technology (Atlanta, GA).

References and Notes

(1) Kresge, C. T.; Leonowicz, M. E.; Roth, W. J.; Vartuli J. C.; Beck, J. S. *Nature* **1992**, *359*, 710.

(2) Beck, J. S.; Vartuli, J. C.; Roth, W. J.; Leonowicz, M. E.; Kresge, C. T.; Schmitt, K. D.; Chu, C. T.-W.; Olson, D. H.; Sheppard, E. W.; McCullen, S. B.; Higgins, J. B.; Schlenker, J. L. *J. Am. Chem. Soc.* **1992**, *114*, 10834.

(3) Luan, Z.; Cheng, C. F.; Zhou, W.; Klinowski, J. *J. Phys. Chem.* **1995**, *99*, 1018.

(4) Luan, Z.; He, H.; Zhou, W.; Cheng C. F.; Klinowski, J. *J. Chem. Soc., Faraday Trans.* **1995,** *91*, 2955.

(5) Schmidt, R.; Akporiaye, D.; Stocker, M.; Ellestad, O. *J. Chem. Soc., Chem. Commun.* **1994**, 1493.

(6) Borade R. B.; Clearfield, A. *Synthesis of Porous Materials: Zeolites, Clays and Nanostructures*; Occelli, M. L., Kessler, H., Eds.; Marcel Dekker Inc.: New York, 1997.

(7) Borade R. B.; Clearfield, A. *Catal. Lett.* **1995**, *31*, 267.

(8) Busio, M.; Janchen, J.; Van Hooff, J. H. C. *Microporous Mater*. **1995**, *4*, 211.

(9) Biz, S.; Occelli, M. L.; Auroux A.; Ray, G. J. Presented at the 15th North American Catalysis Society Meeting in Chicago, May 1997.

(10) Barrett, E. P.; Joyner, L. S.; Halenda, P. P. *J. Am. Chem. Soc.* **1951**, *73*, 373.

(11) Parry, E. P. *J. Catal.* **1963**, *2*, 371.

(12) Hughes, T. R.; White, H. M. *J. Phys. Chem.* **1967**, *71*, 2192.

(13) Parillo, D. J.; Adamo, A. T.; Kokotailo G. T.; Gorte, R. J. *Appl. Catal.* **1990**, *67*, 107.

(14) Biaglow, A. I.; Gittleman, C.; Gorte, R. J.; Madon, R. J. *J. Catal.* **1991**, *129*, 88.

(15) Juskelis, M. V.; Slanga, J. P.; Roberie T. G.; Peters, A. W. *J. Catal.* **1992**, *138*, 391.

(16) Parillo, D. J.; Gorte, R. J. *J. Phys. Chem.* **1993**, *97*, 8786.

(17) Chen, C.-Y.; Li, H.-X.; Davis, M. E. *Microporous Mater.* **1993**, *2*, 17.

(18) Tanev, P. T.; Chlbwe, M.; Pinnavaia, T. J. *Nature* **1994**, *368*, 321.

(19) Kresge, C. T.; Leonowicz, M. E.; Roth, W. J.; Vartuli, J. C. US Patent No. 5098684, 1992.

(20) Mokaya, R.; Jones, W. *J. Chem. Soc, Chem. Commun.* **1997**, 2185.

(21) Branton, P. J.; Hall, P. G.; Sing, K. S. W. *J. Chem. Soc, Chem. Commun.* **1993**, 1257.

(22) Ray, G. J.; Meyers, B. L.; Marshall, C. L. *Zeolites* **1987**, *7*, 307.

(23) Occelli, M. L.; Biz, S.; Auroux, A.; Iyer, P. S. submitted to *Microporous Mesoporous Mater*.

(24) Corma, A.; Fornes, V.; Navarro, M. T.; Perez-Pariente, J. *J. Catal*. **1994**, *148*, 569.

(25) Chen, C.-Y.; Burkett, S. L.; Li, H.-X.; Davis, M. E. *Microporous Mater*. **1993**, *2*, 27.

(26) Huo, Q.; Margolese, D. I.; Ciesla, U.; Demuth, D. G.; Feng, P.; Gier, T. E.; Sieger, P.; Firouzi, A.; Chmelka, B. F.; Schuth, F.; Stucky, G. D. *Chem. Mater.* **1994**, *6*, 1176.

(27) Firouzi, A.; Kumar, D.; Bull, L. M.; Besier, T.; Sieger, P.; Huo, Q.; Walker, S. A.; Zasadzinski, J. A.; Glinka, C.; Nicol, J.; Margolese, D.; Stucky, G. D.; Chmelka, B. F. *Science* **1995**, *267*, 1138.

(28) Iler, R. K. *The Chemistry of Silica*; John Wiley: New York, 1979.

(29) Brinker, C. J.; Scherer, G. W. *Sol−Gel Science: the Physics and Chemistry of Sol−Gel Processing*, Academic Press: Boston, MA; 1990.

(30) Coustel, N.; Di Renzo, F.; Fajula, F. *J. Chem. Soc., Chem. Commun.* **1994**, 967.

(31) Fontell, K.; Khan, B.; Lindstrom, K. B.; Maciejewska D.; Puang-Ngern, S. *Colloid Polym. Sci*. **1991**, *269*, 727.

(32) Vartuli, J. C.; Kresge, C. T.; Roth, W. J.; McCullen, S. B.; Beck, J. S.; Schmitt, K. D.; Leonowicz, M. E.; Lutner, J. D.; Sheppard, E. W. Presented at the American Chemical Society Meeting in Anaheim, CA, April 2−7, 1995.

(33) Edler, K. J., Reynolds, P. A.; White, J. W.; Cookson, D. *J. Chem. Soc., Faraday Trans.* **1997**, *93* (1), 199.